The Temperature-Sensitive *brush* Mutant of the Legume *Lotus japonicus* Reveals a Link between Root Development and Nodule Infection by Rhizobia[C][W][OA]

Makoto Maekawa-Yoshikawa, Judith Müller[1], Naoya Takeda[2], Takaki Maekawa[3], Shusei Sato, Satoshi Tabata, Jillian Perry, Trevor L. Wang, Martin Groth, Andreas Brachmann, and Martin Parniske*

University of Munich, 82152 Munich-Martinsried, Germany (M.M.-Y., J.M., N.T., T.M., M.G., A.B., M.P.); Kazusa DNA Research Institute, Kisarazu, Chiba 292–0818, Japan (S.S., S.T.); and John Innes Centre, Norwich NR4 7UH, United Kingdom (J.P., T.L.W.)

The *brush* mutant of *Lotus japonicus* exhibits a temperature-dependent impairment in nodule, root, and shoot development. At 26°C, *brush* formed fewer nodules, most of which were not colonized by rhizobia bacteria. Primary root growth was retarded and the anatomy of the *brush* root apical meristem revealed distorted cellular organization and reduced cell expansion. Reciprocal grafting of *brush* with wild-type plants indicated that this genotype only affected the root and that the shoot phenotype was a secondary effect. The root and nodulation phenotype cosegregated as a single Mendelian trait and the *BRUSH* gene could be mapped to the short arm of chromosome 2. At 18°C, the *brush* root anatomy was rescued and similar to the wild type, and primary root length, number of infection threads, and nodule formation were partially rescued. Superficially, the *brush* root phenotype resembled the ethylene-related thick short root syndrome. However, treatment with ethylene inhibitor did not recover the observed phenotypes, although *brush* primary roots were slightly longer. The defects of *brush* in root architecture and infection thread development, together with intact nodule architecture and complete absence of symptoms from shoots, suggest that *BRUSH* affects cellular differentiation in a tissue-dependent way.

Legumes can establish root nodule symbiosis (RNS) with rhizobia bacteria, which fix atmospheric nitrogen to ammonium in exchange for carbon and are housed intracellularly within the legume plant root nodule organ (White et al., 2007). In the legume *Lotus japonicus*, the symbiotic interaction with *Mesorhizobium loti* is initiated at root hair cells. Plant root exudates are sensed by rhizobia and stimulate the bacterial production of Nod factor (NF) signaling molecules (Lerouge et al., 1990). NF perception involves the NF receptors NFR1 and NFR5 and leads to rapid physiological and morphological changes, such as membrane depolarization, a rhythmic oscillation of calcium concentration termed calcium spiking, and cytoskeleton rearrangements resulting in root hair deformation (Ehrhardt et al., 1992, 1996; Heidstra et al., 1994; Timmers, 2008). Upon attachment to the root hair tip, rhizobia are entrapped by a process called root hair curling. From a cavern formed by the curled root hair, a tubular-like plant plasma membrane-derived structure, the infection thread (IT), is formed inside the root hair, into which the rhizobia grow by continuous division (Gage, 2004). In parallel, cortical cell divisions are initiated in the root cortex, leading to the development of a nodule primordium. The IT subsequently grows toward the nodule primordium, penetrates into a cortical cell after a cytoplasmic bridge called the preinfection thread was formed, which determines the growth direction of the IT through the cortical cell. Ultimately, the bacteria are released into the plant cell by a process resembling endocytosis. Inside the plant cell cytosol, the bacteria differentiate into bacteroids and form organelle-like symbiosomes that actively fix atmospheric nitrogen.

Initiation of RNS is strictly controlled by the host plant at the level of both plant-assisted rhizobial invasion of the epidermis-derived root hair cell followed by IT formation and development of a nodule primordium in the root cortex. Several different mutants exhibiting a defect in IT and nodule formation have been described phenotypically so far, and a number of genes required for RNS have been isolated (Oldroyd and Downie, 2008). The encoded proteins include receptor kinases, ion channels, nuclear pore

[1] Present address: Ulm University, Institute for General Genetics and Molecular Cytology, James-Franck-Ring, 89069 Ulm, Germany.

[2] Present address: National Institute of Agrobiological Sciences, 2–1–2 Kannondai, Tsukuba, Ibaraki 305–8602, Japan.

[3] Present address: Department of Plant Microbe Interactions, Max-Planck-Institute for Plant Breeding Research, Carl-von-Linné Weg 10, 50829 Cologne, Germany.

* Corresponding author; e-mail parniske@lmu.de.

The author responsible for the distribution of materials integral to the findings presented in this article in accordance with the policy described in the Instructions for Authors (www.plantphysiol.org) is: Martin Parniske (parniske@lmu.de).

[C] Some figures in this article are displayed in color online but in black and white in the print edition.

[W] The online version of this article contains Web-only data.

[OA] Open access articles can be viewed online without a subscription.

www.plantphysiol.org/cgi/doi/10.1104/pp.108.135160

components, transcription factors, an ankyrin repeat membrane protein, and the nuclear-localized protein kinase CCaMK. Mutants in these genes are impaired in nodule formation and ITs are either not formed at all or aborted within the root hair. Interestingly, a gain-of-function mutation in *CCaMK*, encoding a calcium and calmodulin-dependent protein kinase, can trigger development of spontaneous nodules in the absence of rhizobia (Tirichine et al., 2006). Spontaneous nodule development can also be induced by exogenous application of the phytohormone cytokinin and by the gain-of-function mutant *spontaneous nodule formation2* (*snf2*) of the *L. japonicus* cytokinin receptor *Lotus histidine kinase1* (*Lhk1*; Tirichine et al., 2007). Conversely, *L. japonicus hyperinfected1* mutants, which carry a loss-of-function allele of the cytokinin receptor *Lhk1*, are characterized by excessive IT formation upon rhizobia infection, but fail to initiate nodule primordia (Murray et al., 2007). In addition to the symbiosis phenotype, *snf2* mutants display an altered root architecture with extra cell layers (Tirichine et al., 2007). Also, in Arabidopsis (*Arabidopsis thaliana*), cytokinin has an effect on root development by limiting root meristem size and activity (Werner et al., 2001).

These findings and many others provide evidence for obvious links between phytohormone signaling in nodule and root development. Meristematic cells proliferate and differentiate into cells of root and shoots. Although the shoot apical meristem and root apical meristem (RAM) are under distinct genetic regulation, they share the same developmental mechanism for maintaining the stem cells in response to environmental cues (Veit, 2004, 2006). This ability to alter tissue development provides the plasticity necessary for adaptation to various environmental conditions. Initiation of nodule primordia is a typical example for postembryonic development. The legume root nodule is not derived from the RAM, but from fully differentiated cortical cells at the infection site that are rejuvenated and enter mitotic cell divisions. The nodule number per plant is modulated by various environmental and nutrition factors, like availability of nitrogen (Barbulova et al., 2007).

Other essential factors regulating postembryonic development in plants are plant hormones. The spatiotemporal hormone landscape plays a crucial role in the regulation of nodule positioning and the de novo organogenesis in the root. For example, auxin is involved in cell division control, differentiation of lateral roots, as well as in nodule formation (de Billy et al., 2001). In Arabidopsis, overproduction of endogenous ethylene results in the suppression of cell division in the quiescent center, consequently leading to growth reduction of the primary root (Ortega-Martinez et al., 2007). The *Medicago truncatula sickle* mutant forms supernumerical nodules, presumably due to a loss of negative regulation by the plant hormone ethylene. *Sickle* encodes a gene orthologous to Arabidopsis *ETHYLENE INSENSITIVE2*, which is required for ethylene signaling (Penmetsa et al., 2008). Ethylene contributes to the positioning of the nodule on the root (Heidstra et al., 1997). However, in soybean (*Glycine max*), the nodulation phenotype of ethylene-insensitive mutants was indistinguishable from wild type (Schmidt et al., 1999). In *Sesbania rostrata*, ethylene positively acts on infection pocket and nodule primordium formation (D'Haeze et al., 2003). Therefore, the specific role of ethylene in nodulation may vary between different species.

The genetic analysis of intersections between general plant development and nodulation requires the analysis of mutants that are not specifically defective in symbiosis, but show pleiotropic developmental defects. Here, we describe the novel nodulation-deficient *L. japonicus* mutant *brush*. A detailed phenotypic analysis indicated that root growth and bacterial infection were hampered. *BRUSH* is thus not a symbiosis-specific gene, but is also required for proper root development. Pleiotropic mutants like *brush* are invaluable tools to identify the involvement of general plant developmental pathways in nodulation, including hormone regulation. Surprisingly, although root nodule organogenesis was delayed and most nodules were empty, nodule architecture was not affected as such. *brush* reveals a novel link between cell differentiation specifically in the RAM and rhizobial infection.

RESULTS

L. japonicus brush Mutants Exhibit Nodulation and Growth Defects

Line SL0979-2 was isolated as a nodulation-deficient ethyl methanesulfonate mutant of *L. japonicus* accession Gifu (referred to as wild type; Perry et al., 2003). When inoculated with *M. loti* and grown at 26°C, the number of nodules was drastically reduced in the mutant (Fig. 1, A–C). The root hair and calcium spiking responses to NF or *M. loti* were similar to wild type, indicating no defect in early recognition of the bacteria (Supplemental Fig. S1; Supplemental Table S1). We observed normal colonization patterns by *Glomus intraradices* (Supplemental Fig. S2), indicating that arbuscular mycorrhizal symbiosis was not disturbed in the *brush* mutants.

In addition to the nodulation deficiency, *brush* mutants had shorter shoots, shorter primary roots, and red hypocotyls probably due to anthocyanin accumulation (Fig. 1A). The diameter of primary roots was not uniform throughout the length and overall thicker than wild type (Fig. 1, B and C). The number of lateral roots formed on a primary root varied between plants, but, like the primary roots, they were also relatively short (Fig. 1A). Root hairs as well as trichome structure appeared normal (Supplemental Fig. S1B; data not shown). Closer observation of mutant root tips showed that the root apical region was thicker and root hair density was higher (Fig. 1, H and I). Because

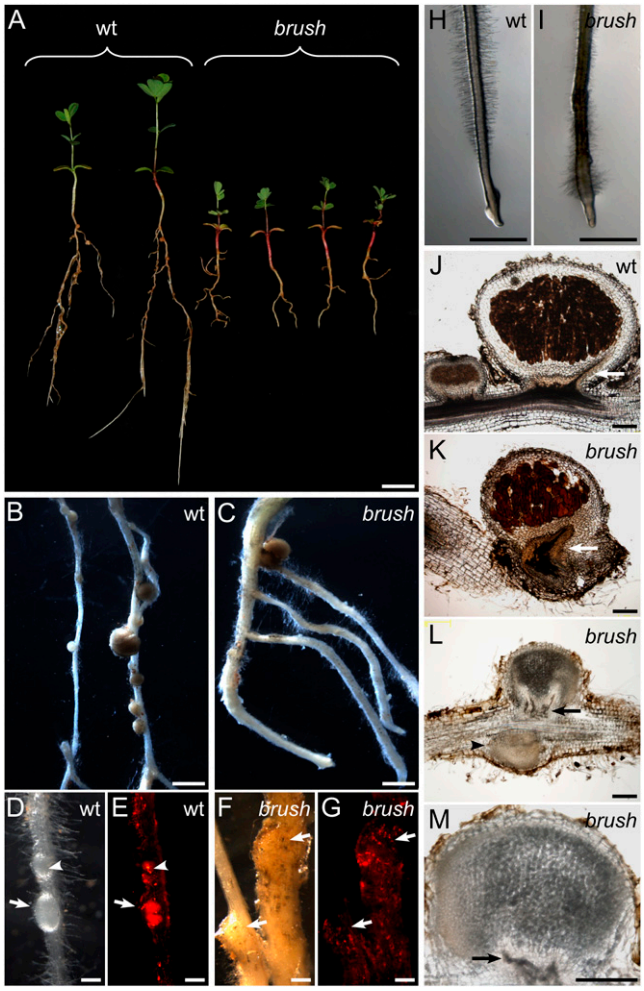

Figure 1. *brush* shoot, root, and nodulation mutant phenotypes. A, *brush* mutant plants display shorter roots and shoots in comparison to wild-type (wt) plants. Stereomicroscopic images of wild-type (B, D, and E) and *brush* (C, F, and G) roots with young developing nodules (arrows) are shown in bright-field (B, C, D, and F) and red fluorescence emission (E and G) microscopy. Inside wild-type nodules, a strong fluorescent signal (E, arrow) and invading ITs (D and E, arrowheads) could be detected, whereas mutant nodule structures (F and G) lack bacterially expressed red fluorescence inside the bump-like structures that were initiated on the root (arrows). Stereomicroscopic images of wild-type (H) and *brush* (I) roots of plants grown in the presence of 0.01 μM AVG for 1 week on agar plates at 26°C. Bright-field microscopic imaging of 40-μm sections of *brush* versus wild-type mature and immature nodules. J, Section of wild-type immature and mature nodules. K, Section of infected mature *brush* nodule. L, Longitudinal section of the typical *brush* aberrant root structure with a nodule and a nodule primordium without bacterial infection (arrowhead), which did not develop any nodule vascular bundle at the base. M, Mature, uninfected *brush* nodule. Arrows in J to M indicate the nodule vascular bundle. B to G and J to M show nodules from plants that were grown for 4 weeks in the presence of *M. loti* MAFF303099 (DsRed) in glass jars at 26°C. Scale bars: 1 cm (A); 2 mm (B, C, H, and I); 200 μm (D–G, J–M).

of the increased root hair density around the root tip, we named the mutant *brush*. All of the nonsymbiotic aspects of the root phenotype were independent of inoculation with *M. loti*.

BRUSH Is a Novel and Single Locus Gene

The three different phenotypes (short root, short shoot, and impaired nodulation) described for the *brush* mutant plants were stably inherited in M_4 and M_5 generations. All F_1 progeny of crosses between *L. japonicus* accession Miyakojima (MG-20) and one M_4 individual of *L. japonicus* Gifu *brush* (internal ZopRA database entry J6900) showed normal plant growth and nodule formation, indicating that the *brush* mutation is recessive. We analyzed 902 self-progeny of these F_1 individuals for cosegregation of the root and nodulation phenotypes. In all clearly scorable cases, the root and nodulation phenotypes occurred together, indicating cosegregation of both traits. We observed 688 (76.3%) wild-type plants and 213 (23.6%) plants mutant for both the nodule and the root phenotype. This suggests that a single locus mutation is responsible for the observed defects. The segregation of phenotypes was also analyzed within the self-progeny of four back-cross individuals (BC1) resulting from two independent back-crosses of *brush* with Gifu wild type. The observed segregation ratio was 74:24 (wild type:*brush*), with clear cosegregation of root and nodule phenotype. Analysis of molecular markers in mutant F_2 individuals derived from the MG-20/*brush* crosses linked the mutant locus to marker TM0312 on the short arm of chromosome 2 (Fig. 2). We identified a total of five mutant recombinants within an interval of $<$0.1 cM around *brush*, all of which showed both low nodulation and short roots. Therefore, we concluded that all mutant phenotypes were caused by a single mutation or very tightly linked mutations.

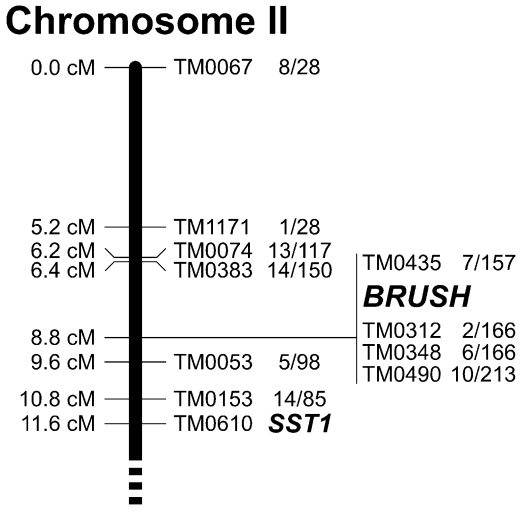

Figure 2. Location of *BRUSH* on the short arm of chromosome 2. Markers and genetic positions are according to Sato et al. (2008). Numbers next to markers indicate the fraction of heterozygous individuals among the total number of *brush*/*brush* homozygotes analyzed. *SST1*, *SYMBIOTIC SULFATE TRANSPORTER1* (Krusell et al., 2005).

The Nodulation Deficiency of *brush* Is Temperature Dependent

Because initial experiments indicated a temperature dependence of the *brush* phenotype, plants were subsequently grown at 18°C and 26°C as permissive and restrictive temperatures, respectively. Inoculation with *M. loti* MAFF 303099 constitutively expressing the DsRed fluorescent protein (MAFF DsRed) allowed us to follow rhizobial infection by fluorescence microscopy.

At 26°C, *brush* mutants formed fewer nodules than wild type (Fig. 1, B and C). Whereas wild-type plants had on average 18 nodules and nodule primordia per root, *brush* mutants had only two (Fig. 3G). Of these, only 15% were infected by bacteria compared to almost 100% in the wild type (Fig. 3I). Although root hair curling appeared normal in *brush* roots, the number of ITs in *brush* was reduced compared to wild type (Fig. 3H). Most of the ITs showed abortion within the root hair cells and only very few reached the next cell layer (Supplemental Fig. S3). In wild-type roots, nodule primordia were round and infected as seen by the bacteria-derived red fluorescence (Fig. 1, D and E), whereas *brush* mutant roots mostly developed irregularly shaped, bump-like structures without visible signs of infection (Figs. 1, F and G, and 3, A–C).

Microscopic analysis of sections of nodules and nodule primordia revealed additional *brush* phenotypes. In wild type, most nodules displayed a brownish color, suggesting bacterial presence and functional nodules (Fig. 1J). In *brush* mutants, only few nodules showed brownish bacteria-containing cells (Fig. 1K). The overall structure of these mature nodules, including vascular bundles and the central tissue, appeared normal when compared to wild-type nodules under both permissive and restrictive conditions (Fig. 1, J and K). However, the majority of nodules on *brush* plants did not contain brownish cells, but still showed clear signs of normal organ differentiation (Fig. 1, L and M). These nodules appeared arrested in development as can be seen by the incomplete differentiation of vascular bundles, most likely due to lack of bacterial infection (Fig. 1, L and M; arrow).

On the other hand, when brush mutants were incubated at 18°C, most nodules resembled those of the wild type. The brownish color was more pronounced in those nodules, and also the vascular bundle surrounded the nodule central tissue as found in wild-

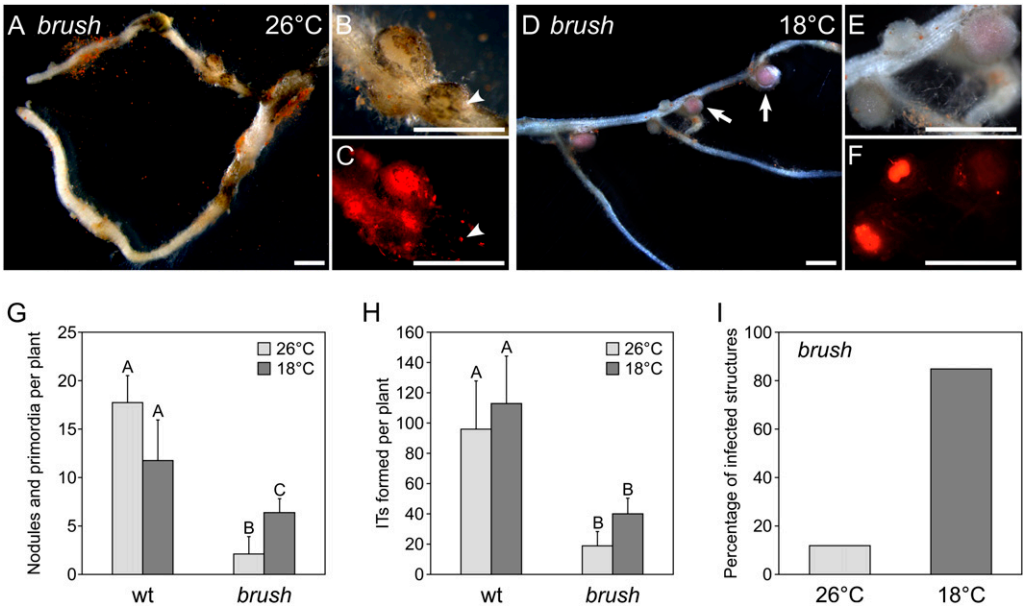

Figure 3. Temperature-dependent *brush* nodulation phenotype. All plants were grown in glass jars for 4 weeks in the presence of *M. loti* MAFF303099 (DsRed). A to F, Stereomicroscopic images showing infected *brush* roots grown at 26°C (A–C) or 18°C (D–F). B and E, Detailed views of A and D, respectively. C and F, Fluorescent microscopic images showing the bacterially expressed red fluorescence upon excitation at 545 nm. In contrast, round pink nodules with vascular bundle formation were apparent (D, arrows) when plants were grown and inoculated at the permissive temperature of 18°C, whereas at 26°C mostly white nodule primordia were observed (A–C). At the root surface, infection events were visible (B and C, arrowheads). Scale bars = 1 mm (A–F). G to I, Growth and nodule kinetics of *brush* plants grown at 18°C versus 26°C. Light gray bars, 26°C; dark gray bars, 18°C. The number of nodules plus nodule primordia (G), and the average of ITs per plant (H) are shown. The percentage of infected nodules and nodule primordia on *brush* roots grown at the two different temperatures is given in I. Values represent the mean and SD of two independent experiments with 15 plants for each condition. Any pairwise comparisons labeled with different letters are significantly different from each other at the 0.05 level as determined by Tukey's honestly significant difference test. wt, Wild type.

type nodules (Fig. 3, D [arrows] and E). After growth at 18°C, a strong bacteria-derived fluorescent signal was observed within nodule primordia and white immature nodules (Fig. 3F), indicating that these not fully mature structures also were infected by rhizobia. The number of ITs on *brush* roots also increased at 18°C compared to 26°C, although this increase was not statistically significant and occurred to a similar extent in wild-type plants (Fig. 3H). Wild-type plants grown at 18°C developed fewer nodules and primordia compared to plants grown at 26°C (Fig. 3G). In contrast, *brush* plants showed a significantly increased number of nodules and primordia at 18°C compared to 26°C. Nevertheless, no full rescue of nodule number up to wild-type level was observed (Fig. 3G). However, at 18°C, the proportion of infected nodules and primordia in *brush* rose almost 6-fold to 86% (Fig. 3I), indicating that the rhizobial infection process in *brush* benefits strongly from growth at the lower temperature.

The *brush* Root Phenotype Is Temperature Dependent

Due to the temperature sensitivity of the symbiotic phenotype, we asked whether the *brush* primary root growth defect was also rescued at lower temperatures. *brush* primary roots were longer at 18°C than at 26°C, but not fully restored to wild-type level (Fig. 4A). Thin sections of roots were analyzed to assess their cellular organization. At 26°C, wild-type roots displayed distinctive and organized cell layers (Fig. 4B). At the meristematic region, called root initial, the putative quiescent center was surrounded by small, actively dividing cells, which later differentiate in the different cell types (Fig. 4B; arrowhead; Supplemental Fig. S4, B and D). These small cells at or near the root initial were filled with cytoplasm, whereas small vacuoles were visible in maturing cells located at the upper distal part of the root initial where cell expansion had occurred (Fig. 4B; arrow). In addition, the root cap region (columella), required for root tip protection, showed uniformly squared, highly enlarged, and longitudinally expanded cells outward in the direction of growth (Fig. 4B; Supplemental Fig. S4, B and D). At the root hair initiation region, all cells were already fully vacuolated and had a regular and longitudinally expanded shape (Fig. 4B; Supplemental Fig. S5A). Epidermal cells were about one-half the diameter of cortical cells and, within each cell layer, cell size was uniform (Supplemental Fig. S5, A and B).

In contrast, in root sections of *brush* grown at 26°C, a distorted organization within the root cell layers with irregularly filed cells was observed (Fig. 4C; Supplemental Figs. S4, E–H, and S5, C and D). Around the root initials, supernumerous cells were present in which vacuolation had already occurred (Fig. 4C; arrowhead). Moreover, the columella cells in *brush* showed no longitudinal expansion (Fig. 4C; Supplemental Fig. S4, F and H). In the root hair region, differentiation into vascular, endodermal, and cortical cell layers was observed, but cells were irregularly shaped and aligned (Supplemental Fig. S5, C and D). A strong effect of *brush* was apparent in the epidermal cell layer, which was not well defined. *brush* epidermal cells appeared much larger than wild type and were radially expanded. Collectively, these developmental defects gave rise to a severely distorted overall root architecture.

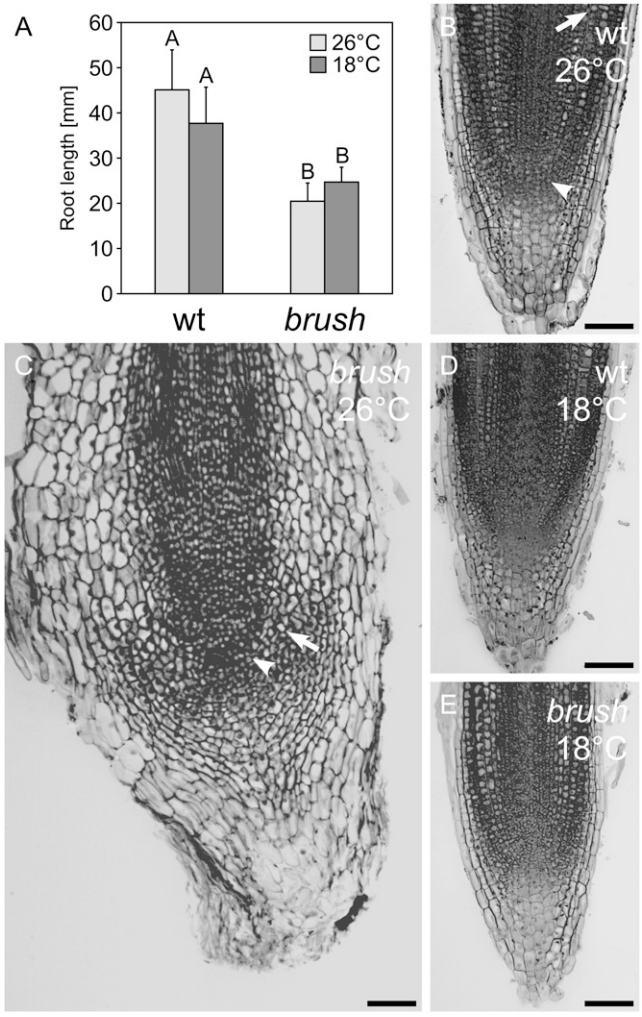

Figure 4. Temperature-dependent *brush* primary root phenotype. All plants were grown in glass jars for 4 weeks in the presence of *M. loti* MAFF303099 (DsRed). A, Root length of wild type and *brush* at 26°C versus 18°C. Values represent the mean and SD of two independent experiments with 15 plants for each condition. Any pairwise comparisons labeled with different letters are significantly different from each other at the 0.05 level as determined by Tukey's honestly significant difference test. Longitudinal RAM sections of wild-type (wt) and *brush* plants at 26°C and 18°C. B, Wild-type root at 26°C. The arrowhead indicates the putative root initial. Vacuole formation is observed in expanded cells in the distal part of the root (arrow). C, *brush* root at 26°C. Vacuolated cells (arrow) were observed very close to the putative root initial (arrowhead), indicating a shortened cell expansion zone. D, Wild-type root at 18°C. E, *brush* root at 18°C. The cell layer differentiation is clearly visible, and cell shape and expansion were completely restored to wild type. Bars = 100 μm.

Wild-type roots grown at 18°C showed no structural differences to roots grown at 26°C, although the overall root length was shorter (Fig. 4, A–D). Surprisingly, at 18°C, *brush* mutant roots showed complete restoration of cellular structure, shape, and size to wild-type levels (Fig. 4, C and E; Supplemental Figs. S4, I–L, and S5, E and F). The putative quiescent center at the root initial became distinctive and the small cells at the surrounding area were filled with cytoplasm and without visible vacuoles. The cells were lined up and underwent cellular expansion, resembling the cell expansion zone of the wild type. The longitudinal root columella cell elongation was restored as well and fully expanded outward (Fig. 4E; Supplemental Fig. S4F). Also, in the root hair region, cells expanded longitudinally similar to wild type (Supplemental Fig. S5E). Transverse sectioning revealed that cell shapes and positions in all cell layers were wild type-like (Supplemental Fig. S5F). This analysis revealed that the root phenotype of *brush* is strongly temperature dependent. The root phenotypes were independent of inoculation with *M. loti* (data not shown).

The *brush* Mutant Phenotype Is Determined by the Root Genotype

To examine whether the *brush* mutant phenotypes were determined by shoot or root genotype, we performed grafting experiments between *brush* and wild-type plants. Two weeks after grafting, the roots were inoculated with *M. loti* MAFF 303099 and nodule formation was analyzed after 4 weeks at 26°C. When wild type as a rootstock was grafted with *brush* as a scion (wild type/*brush*), *brush* shoots grew normal, as did the wild type/wild type grafted plants (Fig. 5, A–C). However, when stock *brush* was grafted with wild-type scion (*brush*/wild type), the shoots looked pale and stunted even 4 weeks after inoculation, probably due to the lack of nodulation of the *brush* roots. This was similar to the situation in *brush*/*brush* grafted plants, which were stunted and non-nodulating (Fig. 5, A–D). On wild-type/*brush* plants, almost the same nodule number was observed as on wild-type/wild-type roots (Fig. 5D), indicating that the *brush* phenotype is root autonomous and determined by the root genotype.

The *brush* Phenotype Is Independent of Ethylene, Abscisic Acid, and GA

The *brush* mutant phenotypes might be due to a difference in production or perception of the plant hormone ethylene, which was found to be a negative regulator of root growth (Ortega-Martinez et al., 2007) and of rhizobial infection (Oldroyd et al., 2001). Therefore, we tested the ethylene responsiveness of the mutants compared to the wild type. *brush* seedlings were subjected to the ethylene precursor 1-aminocyclopropane 1-carboxylic acid (ACC) and grown in the dark. These growth conditions normally

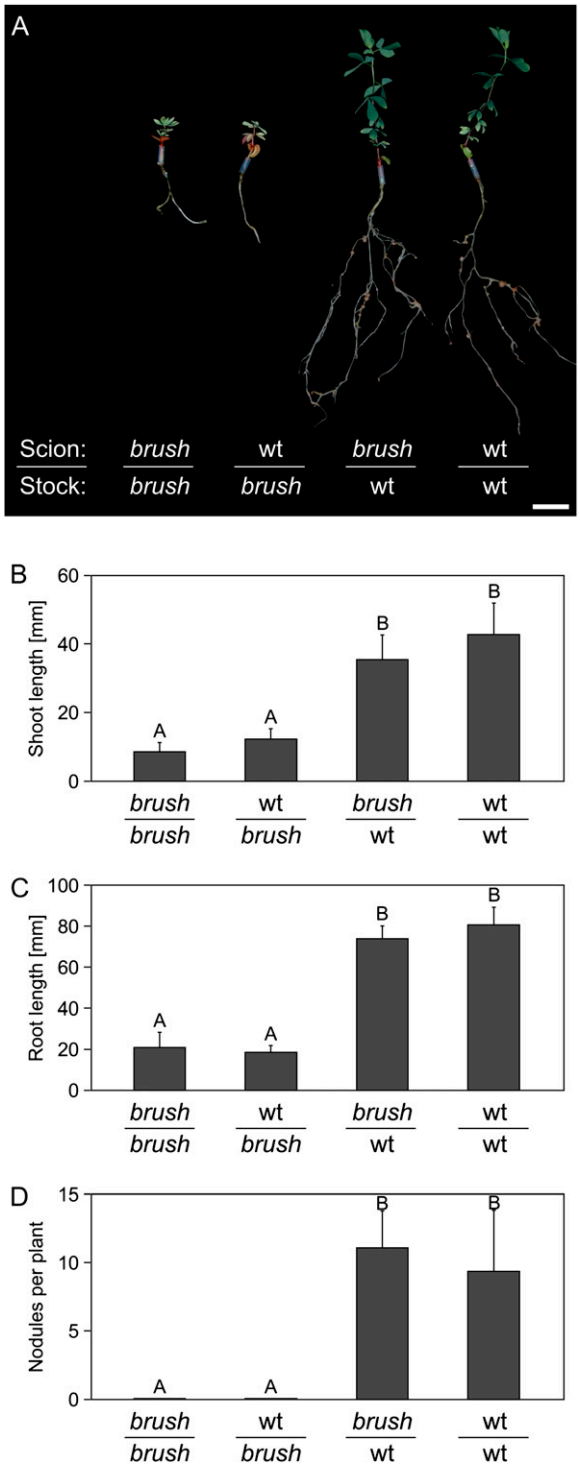

Figure 5. Grafting of *brush* mutants with wild-type (wt) plants. Grafted plants were analyzed 6 weeks after grafting and 4 weeks after rhizobial inoculation. A, Images of grafted plants grown in glass jars. The average shoot (B) and root (C) length and the average number of mature nodules (D) were taken from 17 to 20 plants. Values represent the mean and SD. Any pairwise comparisons labeled with different letters are significantly different from each other at the 0.05 level as determined by Tukey's honestly significant difference test. Bar = 1 cm. [See online article for color version of this figure.]

induce the so-called triple response observed upon etiolating the seedlings (radial swelling of the stem, absence of normal geotropic response, exaggerated apical hook curvature, and inhibition of root and stem elongation; Guzman and Ecker, 1990) in a dose-dependent manner (Fig. 6A). *brush* seedlings showed the same or a slightly higher ethylene sensitivity as the wild type (Fig. 6A), indicating no general defect in ethylene response.

Because the inhibition of primary root growth in *brush* could be caused by excessive endogenous ethylene production, we applied aminoethoxyvinylglycine (AVG), an ethylene synthesis inhibitor, at different concentrations to reduce the endogenous ethylene level. Application of more than 1 μM AVG caused retardation of root growth in both wild type and *brush* (data not shown). Below that concentration, in wild type as well as *brush* plants, root growth was enhanced by the treatment in a dose-dependent manner, although mutant root lengths never reached wild-type levels (Fig. 6B). Thin sectioning of the RAM revealed that AVG treatment did not restore the mutant root architecture back to wild type (Supplemental Fig. S6). We also tested whether the *brush* nodulation defect could be restored by AVG. The different doses of AVG enhanced nodulation in both wild type and *brush* in a similar way, but no apparent recovery of the mutant phenotype to wild-type levels of fully colonized mature nodules was observed (Fig. 6C). We obtained similar results upon silver ion (Ag^+) treatment (Supplemental Fig. S7), which interferes with ethylene perception (Rodriguez et al., 1999).

Other pathways that might be potentially disturbed in *brush* and responsible for the root growth phenotype are abscisic acid (ABA) signaling, exemplified by the *M. truncatula latd* short root mutant (Liang et al., 2007) or the GA pathway. For the latter, a lack of bioactive GA_3 in plants results normally in dwarfism (Koornneef and van der Veen, 1980). However, exogenous application of ABA or GA to *brush* roots failed to rescue the *brush* root mutant phenotype (Supplemental Figs. S8 and S9).

The short root phenotype could also be a consequence of a generally impaired nutritional status. To test this, plants were grown on agar plates containing 1%, 2%, or 4% Suc. Root growth increased in both wild-type and *brush* plants upon addition of Suc in a dose-dependent manner, but mutant root length was never restored to wild-type levels (Fig. 6D) and the root architecture remained disturbed (data not shown). Treatment of roots with 1% mannitol, which influences osmotic regulation, did not enhance growth of either wild-type or *brush* roots (data not shown).

The *brush* Phenotype Is Independent of Auxin

Auxins stimulate cell differentiation, number of lateral roots, and nodule formation (Aloni et al., 2006; Oldroyd and Downie, 2008). Because retardation of root growth and nodulation deficiency in *brush*

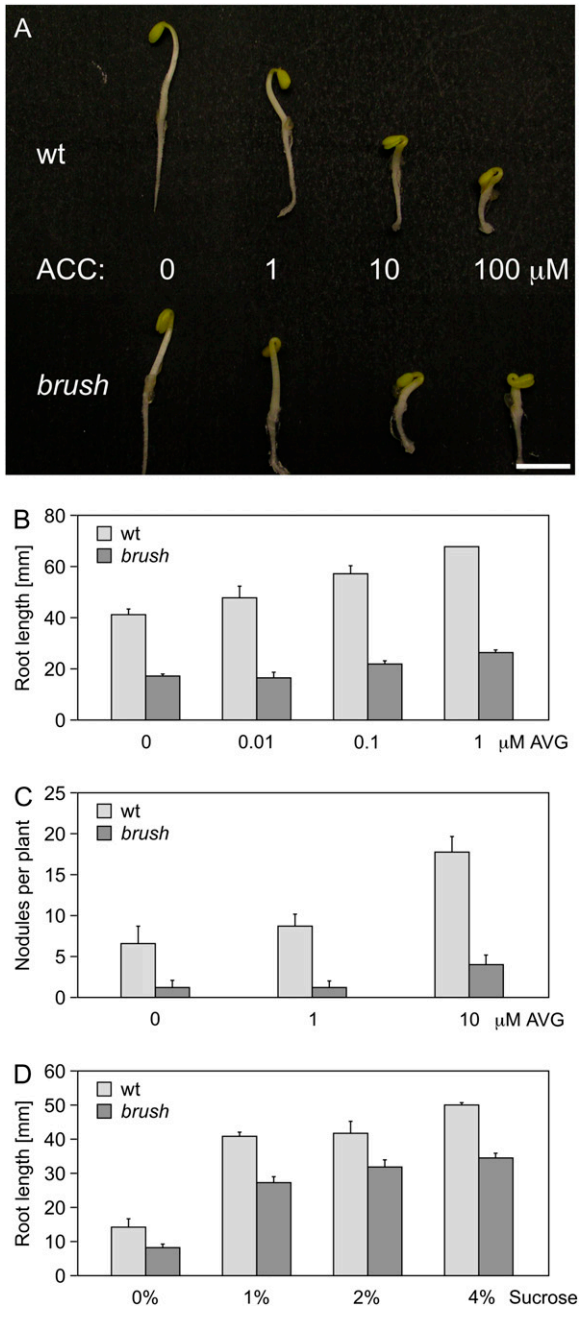

Figure 6. Ethylene and Suc response in *brush* mutants at 26°C. A, Triple response to ACC of *brush* and wild-type (wt) seedlings on half-strength B5 agar plates. B and C, Root length (B) and nodule number (C) of *brush* grown in glass jars for 1 month after addition of different concentrations of AVG compared to wild-type controls. D, Root length of *brush* 5 d after addition of different concentrations of Suc compared to wild-type controls. For A, two independent experiments with at least six individuals per treatment were analyzed; for B, two independent experiments with five individuals per treatment were analyzed. For nodulation experiments in C, each value represents the mean of at least 17 plants; for D, three independent experiments with at least five individuals per treatment grown on half-strength B5 agar plates were analyzed. Values represent the mean and SD. [See online article for color version of this figure.]

could be caused by disturbed auxin homeostasis, plants were subjected to different concentrations of the synthetic auxin analog 1-naphthaleneacetic acid (NAA). When 0.01 μM of NAA was added to wild-type plants, primary root length slightly increased in comparison to nontreated plants, although not significantly (Fig. 7A). At higher NAA concentrations, root growth was inhibited (Fig. 7A). *brush* plants responded to NAA in the same way as wild type (Fig. 7A). However, at 0.01 μM of NAA, no root growth recovery was observed. Addition of NAA also did not lead to a recovery of nodule formation in *brush* (Fig. 7B). Because addition of high concentrations of NAA inhibited root growth, the short root phenotype in *brush* might be caused by overproduction of endogenous auxins. To test this possibility, *brush* plants were treated with the auxin inhibitor 2,3,5-triiodobenzoic acid (TIBA). No significant increase in root length was observed in both wild-type and *brush* roots (Fig. 7C). However, lateral root formation was decreased in both wild type and *brush* in a dose-dependent manner (Fig. 7D), indicating that TIBA was effective in *L. japonicus*.

DISCUSSION

BRUSH Defines a Genetic Link between Cell Differentiation at the RAM and Rhizobial Infection

In this study, we performed a detailed phenotypic analysis of the *L. japonicus brush* mutant, which exhibited three distinctive phenotypes: short root, short shoot, and low number of nodules. Importantly, the majority of nodules were lacking rhizobial infection. We found that the short root phenotype was caused by a severe distortion of the root architecture. *brush* root cells failed to elongate properly and to organize into single files that make up the typical root structure. Interestingly, this differentiation defect was specific for the root. Although rhizobial infection and the frequency of nodule formation were suppressed, the overall architecture of the nodule primordia in *brush* was wild type-like, indicating that cortical cell division and differentiation were not affected. This points to a specific defect that only affects the root architecture, not the initiation of nodule primordia. During microscopic analysis of the *brush* root apical region, the typical root cell layers could still be distinguished, but longitudinal cellular expansion was disturbed. Moreover, grafting experiments revealed that shoot growth could be restored by replacement of mutant with wild-type roots, suggesting that the shoot phenotype is a secondary effect of the root phenotype. We conclude that *brush* exerts a specific effect on cell expansion in the root. Moreover, we could pinpoint the symbiotic defect of brush to the infection of the nodule tissue by rhizobia. These specific defects in *brush* reveal a novel link between cellular development at the root and bacterial infection.

brush Is Temperature Sensitive

The *brush* mutant phenotypes were temperature sensitive: at lower temperatures, root architecture, nodule number, and rhizobial infection were improved. In legumes, several temperature-sensitive mutants have been isolated, such as *sym5* in pea (Fearn

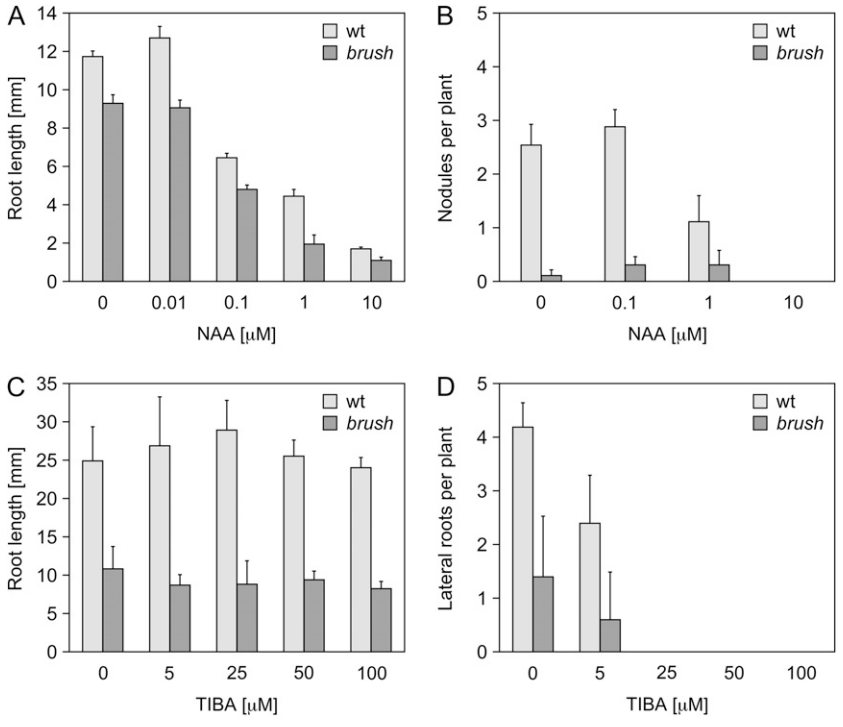

Figure 7. Auxin response in *brush* mutants at 26°C. A, Root length of *brush* 9 d after addition of different concentrations of NAA compared to wild-type (wt) controls. B, Number of nodules formed per plant 14 d after inoculation on different NAA treatments. C and D, Root length (C) and number of lateral roots per plant (D) of *brush* 9 d after addition of different concentrations of TIBA with 2% Suc compared to wild-type controls. In all cases, two independent experiments with at least six individuals per treatment were analyzed. For A, plants were grown on half-strength B5 agar plates; for B, C, and D, plants were grown in glass jars. Values represent the mean and SD.

and LaRue, 1991a) and *nucleoporin133* (*nup133*) and *nup85* in *L. japonicus* (Kanamori et al., 2006; Saito et al., 2007). In our experiments, the lower growth temperature of 18°C did not significantly affect nodule formation in *L. japonicus* Gifu. In contrast, we saw a strong positive effect on *brush* (Fig. 3G), similar to the temperature effect in other temperature-sensitive mutants. It appears unlikely that *brush* is allelic to the *Pisum sativum sym5* mutant because, in this case, nodulation can be recovered by addition of Ag^+ or AVG (Fearn and LaRue, 1991b). *brush* is not an allele of *nup133* or *nup85* because these genes map to chromosome 1 in *L. japonicus*, whereas *brush* is on chromosome 2.

The *brush* Phenotype Differs from That of Previously Described Developmental Mutants of Arabidopsis

Thin sectioning of primary roots of *brush* revealed aberrant root architecture (Fig. 4, B–E). It has been shown previously that growth in the presence of Suc affects the size of the quiescent center (Feldman and Torrey, 1975). Addition of Suc improved primary root growth in *brush* in a dose-dependent manner (Fig. 6, B and D), indicating that in *brush* the quiescent center still holds the ability to respond to Suc. However, root length and root cell architecture were not rescued. *brush* is phenotypically different from some of the CORE (conditional root) mutants in Arabidopsis (Benfey et al., 1993; Hauser et al., 1995) because the phenotypic behavior of the *brush* mutant in Suc was completely opposite from these CORE mutants, where roots show a dose-dependent radial expansion upon Suc treatment. In Arabidopsis, several temperature-dependent mutants have been isolated and characterized (*MICROTUBULE ORGANIZATION1* [*MOR1*] and cellulose synthase [CESA] or related genes; Lane et al., 2001; Whittington et al., 2001; Williamson et al., 2001; Burn et al., 2002a, 2002b). *MOR1*, CESA, and some of the CORE mutants encode genes required for cytoskeleton structural components or their regulation, such as microtubules (MT) and cellulose microfibrils. They are essential components for cell structure and morphology as well as for cell division and cell growth polarity (Sieberer et al., 2005; Paradez et al., 2006; Somerville, 2006; Van Damme et al., 2007; Ishida et al., 2008). For instance, a mutation in *MOR1* led to disruption of the cortical MT network at elevated temperatures (30°C), which then resulted in radial expansion of plant cells in all different plant tissues (Whittington et al., 2001). Furthermore, polar growth of root hairs and trichomes was distorted and *MOR1* obviously plays a crucial role during mitosis and cytokinesis (Whittington et al., 2001; Kawamura et al., 2006). In addition, mutation of *CelA1* (*RSW1*), encoding a protein family member related to cellulose synthases, exhibits a decrease in cell wall cellulose deposition in a temperature-dependent manner (Williamson et al., 2001). This resulted in a similar phenotype as described for *MOR1*. Interestingly, Robledo and colleagues demonstrated that the cell-bound bacterial cellulase CelC2 is essential for the primary infection process in *Rhizobium leguminosarum* (Robledo et al., 2008). These data suggest that cellulytic activity is required for both proper root development and rhizobial infection. It is therefore possible that *BRUSH* encodes a cell wall-modifying enzyme or cytoskeletal component that is specifically required for normal development of the root architecture.

In legumes, rearrangement of the MT is essential for root hair curling, IT formation, and the reentrance into mitosis of cortical cells at the incipient nodule primordium (Timmers, 2008). In contrast to the MT and cellulose mutants mentioned above, which display root hair or trichome defects, the root hair and trichome development of *brush* was normal (Supplemental Fig. S1; Supplemental Table S1; data not shown). Moreover, root hair response to NFs and rhizobia appeared wild type-like. Also, the grafting experiments clearly revealed a root-determined phenotype for *brush* (Fig. 5). Our analysis of arbuscular mycorrhiza development of the *brush* mutant at 26°C did not reveal any differences to wild type (Supplemental Fig. S2). Because penetration of hyphae into the root cortical cell requires proper reorientation and organization of the MT (Genre et al., 2005), these data further support the idea that the cortical MT are not affected in *brush*.

The *brush* Phenotype Appears Independent from the Phytohormones Ethylene, Auxin, ABA, and GA

It is known that plant phytohormones play an important role in plant growth and nodulation. It has been suggested that ethylene directly suppresses cell division in the quiescent center of the RAM, resulting in retarded primary root growth (Ortega-Martinez et al., 2007). Initially, we speculated that the *brush* phenotypes might be caused by the production of, or sensitivity to, ethylene because they resemble typical ethylene-related phenotypes (Fig. 1A). For example, the thick and short root (TSR) syndrome in *Vicia sativa* is characterized by thick and short roots with abundant root hairs very similar to *brush*. However, TSR only develops in the presence of rhizobia or NF (Zaat et al., 1989), whereas in *brush* the root phenotype is independent of NF. The TSR syndrome was found to be ethylene dependent (Zaat et al., 1989). Addition of ACC revealed a clear triple response for *brush* plants as observed for the wild type. Also, treatment with the ethylene synthesis inhibitor AVG did not rescue the root architectural defects in the mutant. In contrast, the previously isolated mutants of *P. sativum*, *sym5*, which is an ethylene hypersensitive mutant (Fearn and LaRue, 1991b), or *sym17* and *sym16*, which are ethylene overproduction mutants (Lee and LaRue, 1992; Guinel and Sloetjes, 2000), displayed a nodulation phenotype rescued by AVG addition. Taken together, these results implied that *BRUSH* exerts an ethylene-independent function.

It has also been suggested that other hormones such as GA and ABA contribute the root elongation and plant growth (Liang et al., 2007) However, addition of GA and ABA on *brush* mutant plants did not recover root development. Auxin hormone landscapes are also crucial for lateral root and nodule primordium initiation and thus auxin signaling might be directly or indirectly affected in *brush*. However, the addition of the synthetic auxin analog NAA did not recover nodule formation or primary root growth in *brush* mutants. Because the number of lateral roots was not altered in *brush* (Fig. 1A), a defect in auxin production or perception seems unlikely. Addition of TIBA, an inhibitor of polar auxin transport, led to a decrease in lateral root formation indicating normal auxin signaling in *brush*, as well. Therefore, we conclude that hormonal disturbances are not the primary cause for the *brush* phenotype.

It has been suggested that gene functions required for nodule formation are recruited from plant developmental pathways (Szczyglowski and Amyot, 2003). Nodulation mutants that show pleiotropic phenotypes, such as *har1*, *astray*, *crinkle*, and *lot1* in *L. japonicus*, and *sickle* and *latd* in *M. truncatula* (Krusell et al., 2002; Nishimura et al., 2002; Tansengco et al., 2003; Oka-Kira et al., 2005; Ooki et al., 2005; Prayitno et al., 2006; Liang et al., 2007), provide evidence for this statement. Our analysis of *brush* reveals a coupled effect on primary root growth and successful rhizobial infection. The combined dataset points to a role of *BRUSH* in determining cell expansion in a tissue or cell type-specific fashion. Cloning of this gene is expected to give deeper insights into the newly discovered relationship between nodule infection and development of the RAM.

MATERIALS AND METHODS

Bacterial Growth and Inoculum Preparation

Mesorhizobium loti MAFF 303099 was obtained from the Ministry of Agriculture, Forestry and Fisheries, National Institute of Agrobiological Sciences, Japan. *M. loti* MAFF 303099 harboring a DsRed, referred to as *M. loti* MAFF DsRed (kindly provided by Dr. M. Hayashi), and wild-type *M. loti* MAFF 303099 strains have been used as rhizobial inoculum for nodulation assays, as well as in root hair deformation analyses. In brief, rhizobia were cultured with TY liquid medium and incubated 2 d in a shaker at 28°C. Rhizobia were then washed with double distilled water three times and suspended in half-strength Broughton & Dilworth (B & D) medium (Broughton and Dilworth, 1971).

Plant Material and Growth Conditions

brush mutant plants were obtained from a population of ethyl methanesulfonate-mutagenized seeds of *Lotus japonicus* B-129 accession Gifu (Perry et al., 2003). All phenotypic analyses were conducted with the M_5 mutant population. Wild-type plants are *L. japonicus* B-129 accession Gifu (Handberg and Stougaard, 1992).

Seeds were germinated upon scarification using sand paper, surface sterilization with 2% (w/v) NaClO for 6 min, and subsequent washing with sterile water, to be finally incubated in water at room temperature for 6 h to overnight, depending on the water absorption of the seeds. Germinated seeds were transferred to 1% (w/v) Bacto agar (GIBCO) prepared in rectangular (18 cm × 18 cm) petri dishes completely wrapped with aluminum foil and incubated in vitro at 16/8-h photoperiods for 2 d, and subsequently subjected to 16/8-h photoperiods for another 2 d without wrapping. For experiments in glass jars, plants were transferred to autoclaved 1-L Weckglass jars containing 250 mL of Seramis (Mars GmbH) and 100 mL of half-strength B & D medium with 100 μM KNO_3. For nodulation analysis, the medium contained rhizobial inoculum to a final OD_{600} of 0.001. Pots were sealed with gas-permeable 3M Micropore surgical tape. Plants were collected 1 month after treatment unless otherwise stated in the text. Nodule images were taken using a Leica MZ 16FA (Leica); for fluorescence microscopy, an RFP filter was used. For experiments on agar plates, plants were grown in petri dishes containing half-strength B5 plant growth medium (Sigma) in 1% Bacto agar (referred to as "half-strength B5 agar plates" in the text). This medium was supplemented with different hormones or other molecules as indicated in the text.

Temperature Sensitivity Analysis

All plants were germinated and planted in sterilized pots as described above. Temperature effects were analyzed by incubation of plants in a temperature-controlled growth chamber with a constant temperature of 26°C or 18°C, with 16/8-h photoperiods.

Grafting of *brush* and Wild-Type *L. japonicus* Plants

Grafting experiments were carried out as described by Nishimura et al. (2002).

Ethylene Sensitivity and Suc Effect Analyses

For triple response analysis, plants were germinated as described above. Two-day-old seedlings were transferred to a half-strength B5 Bacto agar plate containing ACC and incubated at 26°C in the dark for an additional 4 d. For analysis of AVG effects on nodulation and root length, a 10,000× concentrated stock of (S)-trans-2-amino-4-(2-aminoethoxy)-3-butenoic acid hydrochloride (Sigma-Aldrich) was prepared in water and then diluted to the final concentration in the medium supplied to each glass jar. The root length was measured from the junction of hypocotyl and root to the tip of the primary root with digital caliper. Plants were incubated in a growth chamber at 26°C or 18°C with 16/8-h photoperiods. For seedling growth in the presence of Suc, 2-d-old plants were transferred to concentrations of 1%, 2%, and 4% (w/v) Suc in half-strength B5 Bacto agar. The plates were covered up to the plant hypocotyls with a sheet of black paper to avoid direct illumination of the roots. The initial positions of the root tips were marked on the plate. Plates were placed in an upright position and root length was measured from the initial mark to the tip of the primary root.

Auxin Sensitivity Analyses

All plants were germinated and planted in glass jars as described above. 1,000× concentrated stocks of NAA (Sigma-Aldrich) and TIBA (Sigma-Aldrich) were freshly diluted in ethanol and added directly to the liquid medium. Because TIBA inhibits lateral root formation, 2% Suc was added in these experiments to maximize lateral root formation.

Microscopic Analysis of Nodules and Roots

Nodule sections were examined by bright-field microscopy. For this, nodules were freshly harvested and vacuum infiltrated for 20 min with fixation solution (phosphate-buffered saline buffer containing 2.5% [v/v] glutaraldehyde; Sigma-Aldrich) and left at room temperature for about 1 h. Samples were subsequently embedded in 5% (w/v) agarose in water. Vibratome VT1000S (Leica) was used with settings of 40-μm slice thickness, frequency of 2.0, and vibration speed of 2.0. Sections were mounted to glass slides and analyzed using an Olympus BP50 microscope at 5× objective magnification (Olympus).

For examination of RAM architecture, we used the method described in Tansengco et al. (2003). Semithin sections (2–4 μm) were cut from a Technovit 7100 (Heraeus Kulzer) embedded sample block with a Microtome RM 2125RT (Leica). Sections were mounted to glass slides and stained with 0.05% (w/v)

toluidine blue O (SPI Supplies) in Borox buffer at pH 8.4. All these samples were observed with a Leica DMI 6000B at 20× to 40× objective magnification (Leica).

Linkage Analysis

brush was crossed with *L. japonicus* MG-20 accession Miyakojima (Hayashi et al., 2001; Kawaguchi et al., 2001). F_2 progeny were used for linkage analysis. Upon sterilization, seeds were directly planted in Seramis-containing glass jars and inoculated with *M. loti* (final $OD_{600} = 0.001$). One week later the plants were reinoculated with rhizobia. Because mutant plants showed temperature-dependent growth behavior, they were grown at 26°C constantly. Nodulation of the mapping population was checked after 1 month following the first inoculation. The mapping analysis was carried out using simple sequence repeat markers followed by separation on an ABI3730 sequencer allowing further analysis using the GeneMapper software (Applied Biosystems). Simple sequence repeat marker information was obtained from the Kazusa DNA Institute homepage (Sato et al., 2008).

Statistical Analysis

All ANOVA and Tukey's honestly significant difference tests were performed with the Vassar statistical homepage provided by Vassar College. (http://faculty.vassar.edu/lowry/VassarStats.html).

Supplemental Data

The following materials are available in the online version of this article.

Supplemental Figure S1. Root hair morphology of *brush* and wild-type roots.

Supplemental Figure S2. Mycorrhization phenotype of *brush*.

Supplemental Figure S3. IT formation and colonization of root hairs on *brush* plant roots.

Supplemental Figure S4. Temperature-dependent *brush* phenotype at the RAM.

Supplemental Figure S5. Temperature-dependent *brush* phenotype at the root hair zone.

Supplemental Figure S6. AVG treatment of *brush* and wild-type roots.

Supplemental Figure S7. Silver ion treatment of *brush* and wild-type roots.

Supplemental Figure S8. ABA treatment of *brush* and wild-type roots.

Supplemental Figure S9. GA_3 treatment of *brush* and wild-type roots.

Supplemental Table S1. Calcium spiking response in *brush* root hairs.

ACKNOWLEDGMENT

This study is a portion of the dissertation submitted by M.M.-Y. to Osaka University as partial Ph.D. thesis requirement.

Received January 1, 2009; accepted January 23, 2009; published January 28, 2009.

LITERATURE CITED

Aloni R, Aloni E, Langhans M, Ullrich CI (2006) Role of cytokinin and auxin in shaping root architecture: regulating vascular differentiation, lateral root initiation, root apical dominance and root gravitropism. Ann Bot (Lond) **97:** 883–893

Barbulova A, Rogato A, D'Apuzzo E, Omrane S, Chiurazzi M (2007) Differential effects of combined N sources on early steps of the Nod factor-dependent transduction pathway in *Lotus japonicus*. Mol Plant Microbe Interact **20:** 994–1003

Benfey PN, Linstead PJ, Roberts K, Schiefelbein JW, Hauser MT, Aeschbacher RA (1993) Root development in *Arabidopsis*: four mutants with dramatically altered root morphogenesis. Development **119:** 57–70

Broughton WJ, Dilworth MJ (1971) Control of leghaemoglobin synthesis in snake beans. Biochem J **125:** 1075–1080

Burn JE, Hocart CH, Birch RJ, Cork AC, Williamson RE (2002a) Functional analysis of the cellulose synthase genes *CesA1*, *CesA2*, and *CesA3* in Arabidopsis. Plant Physiol **129:** 797–807

Burn JE, Hurley UA, Birch RJ, Arioli T, Cork A, Williamson RE (2002b) The cellulose-deficient *Arabidopsis* mutant *rsw3* is defective in a gene encoding a putative glucosidase II, an enzyme processing N-glycans during ER quality control. Plant J **32:** 949–960

de Billy F, Grosjean C, May S, Bennett M, Cullimore JV (2001) Expression studies on *AUX1*-like genes in *Medicago truncatula* suggest that auxin is required at two steps in early nodule development. Mol Plant Microbe Interact **14:** 267–277

D'Haeze W, De Rycke R, Mathis R, Goormachtig S, Pagnotta S, Verplancke C, Capoen W, Holsters M (2003) Reactive oxygen species and ethylene play a positive role in lateral root base nodulation of a semiaquatic legume. Proc Natl Acad Sci USA **100:** 11789–11794

Ehrhardt DW, Atkinson EM, Long SR (1992) Depolarization of alfalfa root hair membrane potential by *Rhizobium meliloti* Nod factors. Science **256:** 998–1000

Ehrhardt DW, Wais R, Long SR (1996) Calcium spiking in plant root hairs responding to *Rhizobium* nodulation signals. Cell **85:** 673–681

Fearn JC, LaRue TA (1991a) A temperature-sensitive nodulation mutant (*sym5*) of *Pisum sativum* L. Plant Cell Environ **14:** 221–227

Fearn JC, LaRue TA (1991b) Ethylene inhibitors restore nodulation to *sym5* mutants of *Pisum sativum* L. cv Sparkle. Plant Physiol **96:** 239–244

Feldman LJ, Torrey JG (1975) The quiescent center and primary vascular tissue pattern formation in cultured roots of *Zea*. Can J Bot **53:** 2796–2803

Gage DJ (2004) Infection and invasion of roots by symbiotic, nitrogen-fixing rhizobia during nodulation of temperate legumes. Microbiol Mol Biol Rev **68:** 280–300

Genre A, Chabaud M, Timmers T, Bonfante P, Barker DG (2005) Arbuscular mycorrhizal fungi elicit a novel intracellular apparatus in *Medicago truncatula* root epidermal cells before infection. Plant Cell **17:** 3489–3499

Guinel FC, Sloetjes LL (2000) Ethylene is involved in the nodulation phenotype of *Pisum sativum* R50 (*sym16*), a pleiotropic mutant that nodulates poorly and has pale green leaves. J Exp Bot **51:** 885–894

Guzman P, Ecker JR (1990) Exploiting the triple response of *Arabidopsis* to identify ethylene-related mutants. Plant Cell **2:** 513–523

Handberg K, Stougaard J (1992) *Lotus japonicus*, an autogamous, diploid legume species for classical and molecular genetics. Plant J **2:** 487–496

Hauser MT, Morikami A, Benfey PN (1995) Conditional root expansion mutants of *Arabidopsis*. Development **121:** 1237–1252

Hayashi M, Miyahara A, Sato S, Kato T, Yoshikawa M, Taketa M, Hayashi M, Pedrosa A, Onda R, Imaizumi-Anraku H, et al (2001) Construction of a genetic linkage map of the model legume *Lotus japonicus* using an intraspecific F2 population. DNA Res **8:** 301–310

Heidstra R, Geurts R, Franssen H, Spaink HP, Van Kammen A, Bisseling T (1994) Root hair deformation activity of nodulation factors and their fate on *Vicia sativa*. Plant Physiol **105:** 787–797

Heidstra R, Yang WC, Yalcin Y, Peck S, Emons AM, van Kammen A, Bisseling T (1997) Ethylene provides positional information on cortical cell division but is not involved in Nod factor-induced root hair tip growth in *Rhizobium*-legume interaction. Development **124:** 1781–1787

Ishida T, Kurata T, Okada K, Wada T (2008) A genetic regulatory network in the development of trichomes and root hairs. Annu Rev Plant Biol **59:** 365–386

Kanamori N, Madsen LH, Radutoiu S, Frantescu M, Quistgaard EM, Miwa H, Downie JA, James EK, Felle HH, Haaning LL, et al (2006) A nucleoporin is required for induction of Ca^{2+} spiking in legume nodule development and essential for rhizobial and fungal symbiosis. Proc Natl Acad Sci USA **103:** 359–364

Kawaguchi M, Motomura T, Imaizumi-Anraku H, Akao S, Kawasaki S (2001) Providing the basis for genomics in *Lotus japonicus*: the accessions Miyakojima and Gifu are appropriate crossing partners for genetic analyses. Mol Genet Genomics **266:** 157–166

Kawamura E, Himmelspach R, Rashbrooke MC, Whittington AT, Gale KR, Collings DA, Wasteneys GO (2006) MICROTUBULE ORGANIZATION1 regulates structure and function of microtubule arrays during mitosis and cytokinesis in the Arabidopsis root. Plant Physiol **140:** 102–114

Koornneef M, van der Veen JH (1980) Induction and analysis of gibberellin

sensitive mutants in *Arabidopsis thaliana* (L.) Heynh. Theor Appl Genet **58:** 257–263

Krusell L, Krause K, Ott T, Desbrosses G, Kramer U, Sato S, Nakamura Y, Tabata S, James EK, Sandal N, et al (2005) The sulfate transporter SST1 is crucial for symbiotic nitrogen fixation in *Lotus japonicus* root nodules. Plant Cell **17:** 1625–1636

Krusell L, Madsen LH, Sato S, Aubert G, Genua A, Szczyglowski K, Duc G, Kaneko T, Tabata S, de Bruijn F, et al (2002) Shoot control of root development and nodulation is mediated by a receptor-like kinase. Nature **420:** 422–426

Lane DR, Wiedemeier A, Peng L, Hofte H, Vernhettes S, Desprez T, Hocart CH, Birch RJ, Baskin TI, Burn JE, et al (2001) Temperature-sensitive alleles of *RSW2* link the KORRIGAN endo-1,4-beta-glucanase to cellulose synthesis and cytokinesis in Arabidopsis. Plant Physiol **126:** 278–288

Lee KH, LaRue TA (1992) Pleiotropic effects of *sym-17*: a mutation in *Pisum sativum* L. cv Sparkle causes decreased nodulation, altered root and shoot growth, and increased ethylene production. Plant Physiol **100:** 1326–1333

Lerouge P, Roche P, Faucher C, Maillet F, Truchet G, Prome JC, Denarie J (1990) Symbiotic host-specificity of *Rhizobium meliloti* is determined by a sulphated and acylated glucosamine oligosaccharide signal. Nature **344:** 781–784

Liang Y, Mitchell DM, Harris JM (2007) Abscisic acid rescues the root meristem defects of the *Medicago truncatula latd* mutant. Dev Biol **304:** 297–307

Murray JD, Karas BJ, Sato S, Tabata S, Amyot L, Szczyglowski K (2007) A cytokinin perception mutant colonized by *Rhizobium* in the absence of nodule organogenesis. Science **315:** 101–104

Nishimura R, Hayashi M, Wu GJ, Kouchi H, Imaizumi-Anraku H, Murakami Y, Kawasaki S, Akao S, Ohmori M, Nagasawa M, et al (2002) HAR1 mediates systemic regulation of symbiotic organ development. Nature **420:** 426–429

Oka-Kira E, Tateno K, Miura K, Haga T, Hayashi M, Harada K, Sato S, Tabata S, Shikazono N, Tanaka A, et al (2005) *klavier* (*klv*), a novel hypernodulation mutant of *Lotus japonicus* affected in vascular tissue organization and floral induction. Plant J **44:** 505–515

Oldroyd GE, Downie JA (2008) Coordinating nodule morphogenesis with rhizobial infection in legumes. Annu Rev Plant Biol **59:** 519–546

Oldroyd GE, Engstrom EM, Long SR (2001) Ethylene inhibits the Nod factor signal transduction pathway of *Medicago truncatula*. Plant Cell **13:** 1835–1849

Ooki Y, Banba M, Yano K, Maruya J, Sato S, Tabata S, Saeki K, Hayashi M, Kawaguchi M, Izui K, et al (2005) Characterization of the *Lotus japonicus* symbiotic mutant *lot1* that shows a reduced nodule number and distorted trichomes. Plant Physiol **137:** 1261–1271

Ortega-Martinez O, Pernas M, Carol RJ, Dolan L (2007) Ethylene modulates stem cell division in the *Arabidopsis thaliana* root. Science **317:** 507–510

Paradez A, Wright A, Ehrhardt DW (2006) Microtubule cortical array organization and plant cell morphogenesis. Curr Opin Plant Biol **9:** 571–578

Penmetsa RV, Uribe P, Anderson J, Lichtenzveig J, Gish JC, Nam YW, Engstrom E, Xu K, Sckisel G, Pereira M, et al (2008) The *Medicago truncatula* ortholog of *Arabidopsis* EIN2, sickle, is a negative regulator of symbiotic and pathogenic microbial associations. Plant J **55:** 580–595

Perry JA, Wang TL, Welham TJ, Gardner S, Pike JM, Yoshida S, Parniske M (2003) A TILLING reverse genetics tool and a web-accessible collection of mutants of the legume *Lotus japonicus*. Plant Physiol **131:** 866–871

Prayitno J, Rolfe BG, Mathesius U (2006) The ethylene-insensitive sickle mutant of *Medicago truncatula* shows altered auxin transport regulation during nodulation. Plant Physiol **142:** 168–180

Robledo M, Jiménez-Zurdo JI, Velázquez E, Trujillo ME, Zurdo-Piñeiro JL, Ramírez-Bahena MH, Ramos B, Díaz-Mínguez JM, Dazzo F, Martínez-Molina E, et al (2008) *Rhizobium* cellulase CelC2 is essential for primary symbiotic infection of legume host roots. Proc Natl Acad Sci USA **105:** 7064–7069

Rodriguez FI, Esch JJ, Hall AE, Binder BM, Schaller GE, Bleecker AB (1999) A copper cofactor for the ethylene receptor ETR1 from *Arabidopsis*. Science **283:** 996–998

Saito K, Yoshikawa M, Yano K, Miwa H, Uchida H, Asamizu E, Sato S, Tabata S, Imaizumi-Anraku H, Umehara Y, et al (2007) NUCLEOPORIN85 is required for calcium spiking, fungal and bacterial symbioses, and seed production in *Lotus japonicus*. Plant Cell **19:** 610–624

Sato S, Nakamura Y, Kaneko T, Asamizu E, Kato T, Nakao M, Sasamoto S, Watanabe A, Ono A, Kawashima K, et al (2008) Genome structure of the legume, *Lotus japonicus*. DNA Res **15:** 227–239

Schmidt JS, Harper JE, Hoffman TK, Bent AF (1999) Regulation of soybean nodulation independent of ethylene signaling. Plant Physiol **119:** 951–960

Sieberer BJ, Ketelaar T, Esseling JJ, Emons AM (2005) Microtubules guide root hair tip growth. New Phytol **167:** 711–719

Somerville C (2006) Cellulose synthesis in higher plants. Annu Rev Cell Dev Biol **22:** 53–78

Szczyglowski K, Amyot L (2003) Symbiosis, inventiveness by recruitment? Plant Physiol **131:** 935–940

Tansengco ML, Hayashi M, Kawaguchi M, Imaizumi-Anraku H, Murooka Y (2003) *crinkle*, a novel symbiotic mutant that affects the infection thread growth and alters the root hair, trichome, and seed development in *Lotus japonicus*. Plant Physiol **131:** 1054–1063

Timmers ACJ (2008) The role of the plant cytoskeleton in the interaction between legumes and rhizobia. J Microsc **231:** 247–256

Tirichine L, Imaizumi-Anraku H, Yoshida S, Murakami Y, Madsen LH, Miwa H, Nakagawa T, Sandal N, Albrektsen AS, Kawaguchi M, et al (2006) Deregulation of a Ca^{2+}/calmodulin-dependent kinase leads to spontaneous nodule development. Nature **441:** 1153–1156

Tirichine L, Sandal N, Madsen LH, Radutoiu S, Albrektsen AS, Sato S, Asamizu E, Tabata S, Stougaard J (2007) A gain-of-function mutation in a cytokinin receptor triggers spontaneous root nodule organogenesis. Science **315:** 104–107

Van Damme D, Vanstraelen M, Geelen D (2007) Cortical division zone establishment in plant cells. Trends Plant Sci **12:** 458–464

Veit B (2004) Determination of cell fate in apical meristems. Curr Opin Plant Biol **7:** 57–64

Veit B (2006) Stem cell signalling networks in plants. Plant Mol Biol **60:** 793–810

Werner T, Motyka V, Strnad M, Schmulling T (2001) Regulation of plant growth by cytokinin. Proc Natl Acad Sci USA **98:** 10487–10492

White J, Prell J, James EK, Poole P (2007) Nutrient sharing between symbionts. Plant Physiol **144:** 604–614

Whittington AT, Vugrek O, Wei KJ, Hasenbein NG, Sugimoto K, Rashbrooke MC, Wasteneys GO (2001) MOR1 is essential for organizing cortical microtubules in plants. Nature **411:** 610–613

Williamson RE, Burn JE, Birch R, Baskin TI, Arioli T, Betzner AS, Cork A (2001) Morphology of *rsw1*, a cellulose-deficient mutant of *Arabidopsis thaliana*. Protoplasma **215:** 116–127

Zaat S, van Brussel A, Tak T, Lugtenberg B, Kijne J (1989) The ethylene inhibitor aminoethoxyvinylglycine restores normal nodulation by *Rhizobium leguminosarum* biovar. *viciae* on *Vicia sativa* subsp. *nigra* by suppressing the 'thick and short roots' phenotype. Planta **177:** 141–150